

This is the accepted manuscript made available via CHORUS. The article has been published as:

Magnetic interlayer coupling between antiferromagnetic CoO and ferromagnetic Fe across a Ag spacer layer in epitaxially grown CoO/Ag/Fe/Ag(001)

Y. Meng, J. Li, P.-A. Glans, C. A. Jenkins, E. Arenholz, A. Tan, J. Gibbons, J. S. Park, Chanyong Hwang, H. W. Zhao, and Z. Q. Qiu

Phys. Rev. B **85**, 014425 — Published 23 January 2012

DOI: [10.1103/PhysRevB.85.014425](https://doi.org/10.1103/PhysRevB.85.014425)

Magnetic interlayer coupling between antiferromagnetic CoO and ferromagnetic Fe across a Ag spacer layer in epitaxially grown CoO/Ag/Fe/Ag(001)

Y. Meng,^{1,2} J. Li,² P.-A. Glans,³ C.A. Jenkins,³ E. Arenholz,³ A. Tan,² J. Gibbons,² J. S. Park,² Chanyong Hwang,⁴ H. W. Zhao,¹ and Z. Q. Qiu²

¹ Institute of Physics, Chinese Academy of Science, Beijing, 100190, P. R. China

² Department of Physics, University of California at Berkeley, Berkeley, California 94720, USA

³ Advanced Light Source, Lawrence Berkeley National Laboratory, Berkeley, California 94720, USA

⁴ Korea Research Institute of Standards and Science, Yuseong, Daejeon 305-340, Korea

Abstract

CoO/Ag/Fe/Ag(001) films were grown epitaxially and studied using Magneto-Optic Kerr Effect and X-ray Magnetic Circular Dichroism (XMCD). Instead of exponential decay as reported in previous works, we find that both the exchange bias and the coercivity in the epitaxially grown films exhibit a non-monotonous behavior with the Ag spacer layer thickness. By purposely increasing the film roughness, the non-monotonous interlayer coupling evolves into a monotonic decrease with increasing the Ag thickness. Furthermore, we show that the interlayer coupling peak diminishes or shifts its peak position by inserting a Cr layer between CoO and Ag.

PACS numbers: 75.70.Ak

1. Introduction

Ferromagnet(FM)/antiferromagnet (AFM) layered structures have attracted great interest in the last few decades because of the exchange bias [1] effect and its application in spintronics technology [2]. Early explanations of the exchange bias adapted over-simplified AFM spin structures [3,4,5,6] and were soon replaced by more sophisticated models which account for the realistic experimental systems [7,8,9]. While it is clear that it is the AFM layer that induces the exchange bias [10], the AFM/FM magnetic coupling mechanism remains obscure because of the complexity of the magnetic frustration at the interface [2]. In experiment, most of the studies are focused on the direct AFM/FM interfacial coupling, aiming to understand how the interfacial frustration generates the FM layer properties such as the pinning effect [11,12,13], training effect [14,15,16], and the finite size effect [17], etc. One interesting discovery of these studies are that the effect of the AFM layer to the FM layer is determined not only by the AFM spins at the interface but also by the AFM spins deeply inside the AFM layer [18,19,20], suggesting that the exchange bias may have a long-range character. An alternative approach to address the AFM/FM interaction length scale is to insert a nonmagnetic spacer layer between the AFM and the FM layers so that the frustration due to the nearest neighbor AFM spins can be averaged out to certain degree. For metallic AFM layers, Thomas et al. found that both the exchange bias and the coercivity in $\text{Ir}_{22}\text{Mn}_{78}/\text{metal}/\text{Fe}_{16}\text{Co}_{16}$ decrease exponentially with a decay length of only a few angstroms in the spacer layer [21]. Using an ultrahigh vacuum (UHV) system to grow better samples, Mewes et al. found that the exchange bias in $\text{Fe}_{20}\text{Ni}_{80}/\text{Cu}/\text{Fe}_{50}\text{Mn}_{50}$ not only has a long-range character but also oscillates with the Cu spacer thickness with the same mechanism as in FM/metal/FM trilayers [22]. As it is well known, electrons at the Fermi level of a metallic FM/metal/FM system form spin-dependent quantum well states in the spacer layer to mediate a magnetic interlayer coupling between the two metallic FM layers [23]. Then the result of Ref. 22 indicates that a metallic AFM layer should couple to the spacer layer electrons in the same manner as a metallic FM layer. For an insulating AFM layer (e.g., CoO), however, the exchange bias shows a peculiar dependence on the spacer layer thickness. Gökemeijer et al. found that the exchange bias in $\text{CoO}/\text{metal}/\text{Py}$ has an exponential decay with the spacer layer thickness but with a long-range character of as much as 50\AA [24]. However, another experiment on the $\text{CoO}/\text{Au}/\text{Co}$ system shows an abrupt and not a gradual exponential reduction of the exchange bias with Au thickness [25]. Recognizing that the exchange bias

may not be the best quantity to represent the AFM/FM magnetic coupling across a spacer layer, Valev et al. performed magnetization-induced optical second harmonic generation (MSHG) on the CoO/Cu/Fe system and shows that the CoO magnetic order contributes to the MSHG signal even after the exchange bias vanishes [26], favoring the long-range character of the CoO/metal/FM coupling reported in Ref. 24. Despite the above progress, the experimental observation raises a critical question of if there exists an oscillatory coupling in the CoO/metal/FM system as observed in metallic AFM case? The question is raised because CoO is a Mott insulator whose antiferromagnetic order comes from virtual hopping of electrons between nearest neighbors. This insulating AFM character is different from metallic AFM so that in principle it should exhibit a different CoO/metal/FM magnetic coupling compared to the metallic AFM/metal/FM case. In FM/metal/FM systems, the exponential decay of the interlayer magnetic coupling with spacer layer thickness is possible only if the spacer layer processes local electronic states in the vicinity of the Fermi level [27]. Therefore if the CoO/metal/FM interlayer coupling behaves differently from the metallic AFM/metal/FM system, does it imply that the insulating AFM CoO layer induces a local electronic state near the Fermi level of the spacer layer? If this were true, the existing exchange bias models have to be separated into two groups to deal with insulating and metallic AFM layers differently. There has been much effort devoted recently to the CoO/metal/FM system but the evidence of the oscillatory coupling with the spacer layer thickness is rather weak [28,29,30]. Is this due to the Mott insulating nature of CoO or something else (e.g., film roughness or morphology)? Obviously, it becomes an important issue to clarify the existence/absence of the oscillatory CoO/metal/FM interlayer coupling with the spacer layer thickness. In this paper, we report an experimental study of epitaxially grown CoO/Ag/Fe/Ag(001) single crystalline thin films. We show strong evidence of the non-monotonous interlayer coupling between CoO and Fe layers across the Ag spacer layer. By growing samples with different film roughness, we show that the non-monotonous behavior exists only on epitaxial smooth films and diminishes rapidly with increasing film roughness.

2. Experiment

A Ag(001) single crystal substrate was prepared by mechanical polishing down to a 0.25- μm diamond-paste finish, followed by chemical polishing [31]. The Ag substrate was cleaned in an UHV system by cycles of Ar ion sputtering at $\sim 2\text{keV}$ and annealing at 600°C .

An Fe film was grown on top of the Ag(001) substrate, followed by a Ag wedge, and a CoO layer. All films were grown at room temperature of the substrate, and the CoO film was grown by evaporating Co under an oxygen pressure of 1×10^{-6} Torr. The formation of the Low Energy Electron Diffraction (LEED) confirms the epitaxial growth of single crystalline CoO/Ag/Fe films on Ag(001) substrate [Fig. 1(a)]. As reported previously [32], the Fe film on Ag(001) has the bcc structure with the Fe [100] axis parallel to the Ag [110] axis and CoO film has the rock salt structure with the CoO [100] axis parallel to the Ag [100] axis. The sample is covered by a 2nm Ag protection layer and then measured using Magneto-Optic Kerr Effect (MOKE) and X-ray Magnetic Circular Dichroism (XMCD) at the beamline 6.3.1 of the Advanced Light Source (ALS) of the Lawrence Berkeley National Laboratory.

3. Result and Discussion

The sample of CoO(5nm)/Ag/Fe(15ML)/Ag(001) (sample 1 in Table 1) was cooled down to 80K with an external magnetic field applied along the Fe[100] in-plane easy magnetization axis. Since our MOKE magnet can only reach 1.2 kOe, the field cooling and hysteresis loop measurement was accomplished using MOKE for magnetic field less than 1.2 kOe and using XMCD for magnetic field greater than 1.2 kOe. In the XMCD measurement, the x-ray is circularly polarized and is at 60 degree incident angle to the sample surface normal direction so that the projection of the x-ray along the in-plane Fe magnetization direction picks up the Fe XMCD signal. Fig. 2(a) shows the hysteresis loops of CoO(25ML)/Ag/Fe(15ML)/Ag(001) at different Ag spacer layer thicknesses (d_{Ag}), where the loop was obtained using XMCD for $d_{\text{Ag}} < 3\text{ML}$ and using MOKE for $d_{\text{Ag}} \geq 3\text{ML}$. The exchange bias has an obvious long-range character with an exchange bias of $H_E = 98.5$ Oe even at $d_{\text{Ag}} = 17\text{ML}$, confirming the long-range character of exchange bias as reported in Ref. 24. Instead of exponential decay of the exchange bias, we clearly observe a non-monotonous exchange bias with increasing the Ag spacer thickness [Fig. 2(b)]: the exchange bias has a value of $H_E = 380.5$ Oe at $d_{\text{Ag}} = 0\text{ML}$, decreases rapidly to $H_E = 97.5$ Oe at $d_{\text{Ag}} = 3\text{ML}$, increases to $H_E = 278.5$ Oe at $d_{\text{Ag}} = 10\text{ML}$, and then decreases slowly at $d_{\text{Ag}} > 10\text{ML}$. In fact the non-monotonous H_E is so obvious that one can easily identify it even from the hysteresis loops shown in Fig. 2(a). Note that the exchange bias depends on the cooling field history thus is not the best quantity to describe the AFM/spacer/FM interlayer coupling, we then use the FM layer coercivity (H_C) as a better quantity to describe the

AFM/FM coupling [2]. In fact the Fe coercivity of $H_C \sim 1800$ Oe in CoO/Fe is not only much greater than the Fe film itself (~ 100 Oe) but also independent on the cooling history in our CoO/Ag/Fe/Ag(001) system. Therefore we switched our focus on the H_C vs d_{Ag} measurement with or without field cooling after identifying the non-monotonous exchange bias shown in Fig. 2. The result of H_C from CoO(25ML)/Ag/Fe(15ML)/Ag(001) is shown in Fig. 3(a) which clearly reveals the non-monotonous behavior of the CoO/Ag/Fe interlayer coupling.

What is the reason for the appearance of the non-monotonous behavior in our sample? Is it due to the high quality of the epitaxial growth sample or something else? The chemical composition and impurity level could affect the interlayer coupling thus to modify the exchange bias and coercivity of the Fe film. If it were this case, the likely cause would be the growth of CoO that the oxygen ambient pressure oxidizes the films. Indeed it was shown that CoO growth directly on top of Fe film will lead to a monolayer FeO formation at the interface [33,34]. In our case, however, the CoO film is grown on top of the Ag spacer layer. Therefore the Fe film is protected from the oxygen exposure during the CoO growth except in the monolayer regime of the Ag thickness. Indeed the Fe absorption spectrum is metallic-like rather than FeO like above ~ 5 ML Ag. If there were any possibility of chemical composition inhomogeneity, it should be the chemical composition variation of the CoO film at different Ag thicknesses to cause the non-monotonous interlayer coupling. To be certain of this assertion, we measured the Co X-ray Absorption Spectrum (XAS) at the 2p level as a function of Ag thickness. As shown in Fig. 4, the Co XAS exhibits the well-known L_2/L_3 peaks. In particular, the Co L_3 peak splits into a doublet at 775.8 eV and 776.8 eV which is a characteristic feature of the CoO absorption spectrum [35]. Most importantly, the Co XAS does not change with increasing Ag thickness, indicating that the CoO chemical composition is rather uniform with increasing the Ag thickness. Therefore the non-monotonous CoO/Ag/Fe interlayer magnetic coupling is not due to any chemical composition change of the CoO film with increasing the Ag thickness.

We believe that it is the interfacial roughness that is responsible for the absence of the non-monotonous CoO/metal/FM interlayer coupling in previous works. CoO usually does not grow as nicely as metallic films on Ag (e.g., Fe on Ag), leading to a rougher CoO/Ag interface than Fe/Ag. This is partially reflected by the broader CoO LEED spots as compared with Ag LEED spots in Fig. 1. To verify this speculation, we synthesized another 3 samples to gradually increase the film roughness (sample 2-4 in Table 1).

Sample 2 was grown on the same Ag(001) substrate but only with 3-5 cycles of sputtering and annealing. Therefore the Ag(001) substrate in sample 2 is not as flat as the Ag(001) substrate in sample 1 which was after many cycles of sputtering and annealing. However, sample 2 is still a single crystalline epitaxial film of good quality. In fact, we could not see any difference in LEED pattern of sample 2 as compared to sample 1 (not shown Fig. 1). Therefore roughness of sample 2 is beyond the resolution of LEED so it could only be slightly rougher than sample 1. Sample 3 and 4 were grown with a thin Co seed layer on Ag(001). It is known that Co grows on Ag(001) to form a metastable body-centered tetragonal structure for the first few monolayers and then relax into polycrystalline films at higher thickness [36]. Therefore the addition of the Co seed layer is expected to increase the film roughness from sample 2 to sample 3 and to sample 4. Indeed, the LEED pattern of sample 3 [Fig. 1(b)] shows broader LEED spots for Co, Fe, and Ag films with no LEED spot for the CoO film, and sample 4 shows a complete absence of the LEED spot because of polycrystalline formation. Therefore we obtained the CoO/Ag/Fe films with increasing film roughness from sample 1 to sample 4 although we are lack of a quantitative analysis of the film roughness. The coercivities of the sample 2-4 were then measured and the result is shown in Fig. 3. As compared to the H_C of sample 1, all samples 2-4 have a monotonic decrease of the H_C with increasing the Ag thickness. Moreover, as the film roughness increases from sample 2 to 4, the H_C value becomes smaller and smaller at thicker Ag thickness. Therefore the result of Fig. 3 shows that it is the film roughness that diminishes the non-monotonous CoO/Ag/Fe interlayer coupling and makes the interlayer coupling more and more short-range like. This also explains why the absence of the second peak in H_C because the film should become rougher at thicker Ag thickness. It should be mentioned that the absence of the non-monotonous H_C in sample 2 shows that the non-monotonous interlayer coupling in CoO/Ag/Fe is very sensitive to the film roughness. Non-wedged samples and polycrystalline samples could easily diminish the non-monotonous interlayer coupling.

After verifying the existence of the non-monotonous CoO/Ag/Fe interlayer magnetic coupling, we further addressed the coupling nature at the CoO/Ag interface. A sample of CoO(25ML)/Cr/Ag/Fe(20ML)/ Ag(001) was grown (Sample 5 in Table 1) with the Cr film growing into a wedge orthogonal to the Ag wedge. In this sample the AFM/Ag interfacial coupling is gradually changed from CoO/Ag to Co/Cr/Ag across the Cr wedge. The coercivity of the sample is determined by hysteresis loop measurement at

different thicknesses of Cr. As the Cr thickness (d_{Cr}) increases, the H_C peak magnitude at $d_{Ag}=10\text{ML}$ decreases and eventually disappears at $d_{Cr}>3\text{ML}$. This is expected because Cr does not grow as smoothly as Fe on Ag(001) [37] so that the Cr/Ag interfacial roughness should increase with Cr thickness to diminish the H_C peak.

In terms of electronic structure, the spacer layer changes from Ag to Cr/Ag after adding the Cr layer. Then the interesting question is if the diminishment of the H_C peak at $d_{Ag}=10\text{ML}$ is due to a reduction of the coupling strength or a shift of the peak position to thicker Ag thicknesses? At $d_{Cr}=8\text{ML}$, Fig. 5 shows somewhat a peak-like feature at $d_{Ag}=18\text{ML}$. However, this “peak feature” is too weak to be conclusive. Here we would like to discuss a ferromagnetic metallic system to obtain a possible mechanism. For ferromagnetic metallic systems, interlayer coupling is mediated by quantum well states (QWS) in the spacer layer [38,39]. Specifically, QWS in Ag/Fe(001) and Cr/Fe(001) have been studied by a great extent in momentum space using Angle Resolved Photoemission Spectroscopy (ARPES) [40,41]. The result shows that the long- and short-period oscillatory interlayer couplings are associated with QWS at different locations in k-space. When two spacer layers are joined together as in our case, electrons crossing the interface have to conserve their momentum parallel to the interface. This constraint eliminates some QWS in mediating the interlayer coupling. Although no direct measurement has been performed on Cr/Ag(001) spacer layer, interlayer coupling study on a similar system of Fe/Cr/Au/Fe(001) shows that the effect of momentum conservation parallel to the Cr/Au interface is to suppress the long-period interlayer coupling in the Cr layer [42]. That could explain why the coupling peak in Fig. 5 decreases so rapidly with increasing the Cr thickness because the 2ML short-period interlayer coupling is not expected to exist in our systems due to the film roughness. Another mechanism is that the coupling peak position could shift to another film thickness as the second spacer layer is inserted [43]. Unfortunately the H_C peak diminishes so rapidly in our sample that it is difficult to trace the peak position shift reliably beyond 3ML Cr thickness. Although Fig. 5 shows somewhat weak evidence of such shift to $\sim 17\text{-}18\text{ML}$ of Ag at 8ML Cr, the variation of the coercivity is too small to claim it confidently. Therefore we leave it as a possible explanation rather than a conclusion. The last possibility is that the coercivity in CoO/Cr/Ag/Fe/Ag(001) is mainly determined by the coupling between the antiferromagnetic Cr layer and the ferromagnetic Fe layer across the Ag spacer layer. In this case, we would expect a similar H_C behavior in Co/Ag/Fe/Ag(001) and Cr/Ag/Fe/Ag(001). However, the absence of the

oscillatory H_C in CoO/Cr/Ag/Fe/Ag(001) with Ag thickness indicates that it is unlikely that the H_C in CoO/Cr/Ag/Fe/Ag(001) is associated to the coupling between the antiferromagnetic Cr layer and the ferromagnetic Fe layer.

4. Summary

In summary, we find strong evidence of the non-monotonous magnetic coupling between CoO and Fe films across a Ag spacer layer in epitaxially grown CoO/Ag/Fe/Ag(001). We also find that the non-monotonous interlayer coupling disappears by increasing the film roughness, showing that the absence of the non-monotonous interlayer coupling in CoO/metal/FM in previous works is due to film roughness rather than the insulating property of the AFM CoO film. Furthermore we show that inserting a Cr layer between CoO and Ag suppresses the coupling peak at 10ML Ag. This could be due to an increased film roughness, reduction of the long-period coupling in Cr layer, or a phase shift of the coupling to thicker Ag thickness.

Acknowledgement

This work was supported by National Science Foundation DMR-0803305, U.S. Department of Energy DE-AC02-05CH11231, and KICOS through Global Research Laboratory project of Korea.

Table 1: Film roughness increases from Sample 1 to Sample 4.

Sample 1	CoO(25ML)/Ag/Fe(15ML)/Ag(001)	Many cycles of sputtering and annealing of the Ag substrate
Sample 2	CoO(25ML)/Ag/Fe(20ML)/Ag(001)	Only 3-5 cycles of sputtering and annealing of the Ag substrate
Sample 3	CoO(25ML)/Ag/Fe(20ML)/Co(3ML)/Ag(001)	Many cycles of sputtering and annealing of the Ag substrate
Sample 4	CoO(25ML)/Ag/Fe(20ML)/Co(15ML)/Ag(001)	Many cycles of sputtering and annealing of the Ag substrate
Sample 5	CoO(25ML)/Cr/Ag/Fe(20ML)/ Ag(001)	Many cycles of sputtering and annealing of the Ag substrate

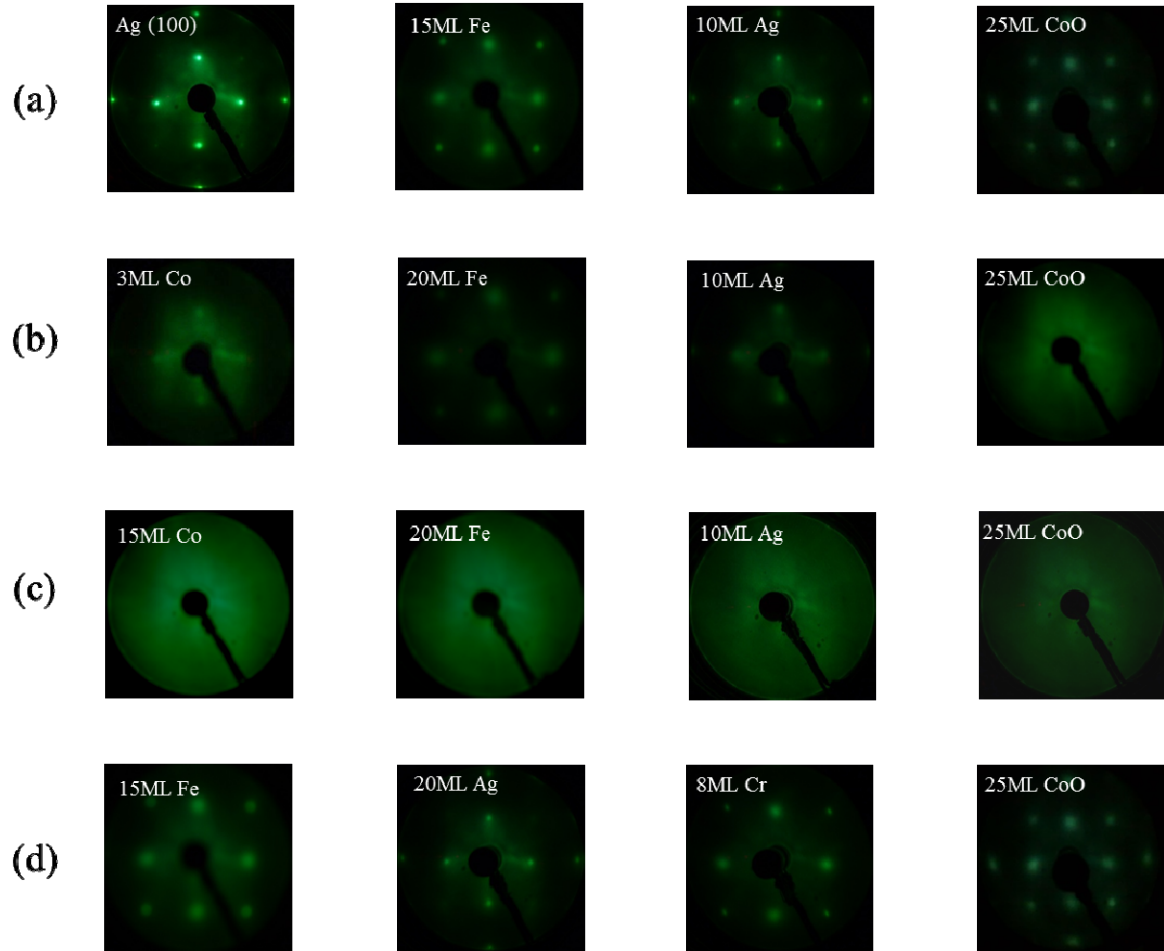


Fig. 1: (color online) LEED patterns at different stages of (a) Sample 1, (b) Sample 3, (c) Sample 4, and (d) Sample 5. The LEED patterns are taken at 123eV for Ag, 91eV for Fe, 123eV for Co, and 91eV for Cr.

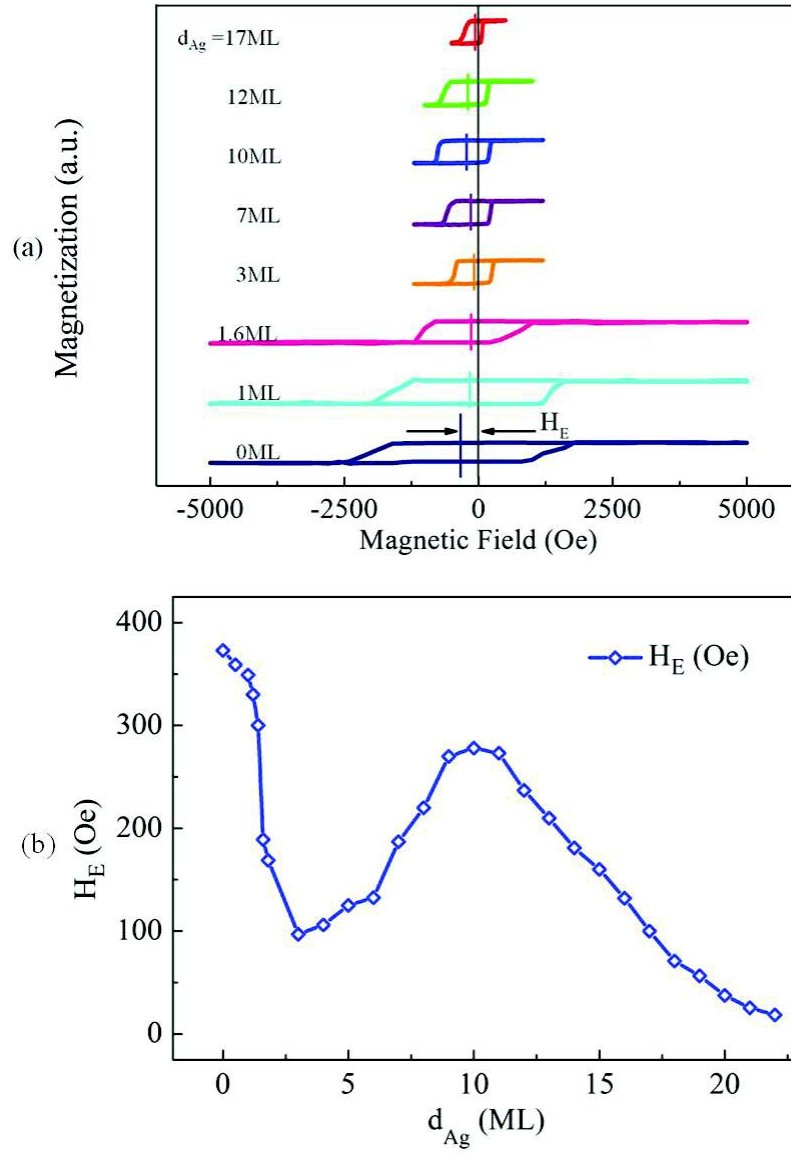


Fig. 2: (color online) (a) Hysteresis loops and (b) exchange bias of sample 1 as a function of the Ag spacer layer thickness.

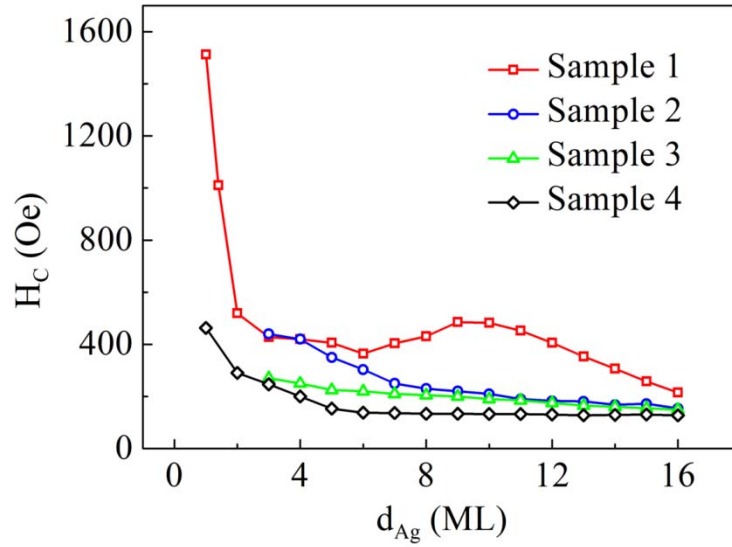


Fig. 3: (color online) Coercivity versus Ag thickness for samples 1-4. The non-monotonous behavior disappears as the film roughness increases.

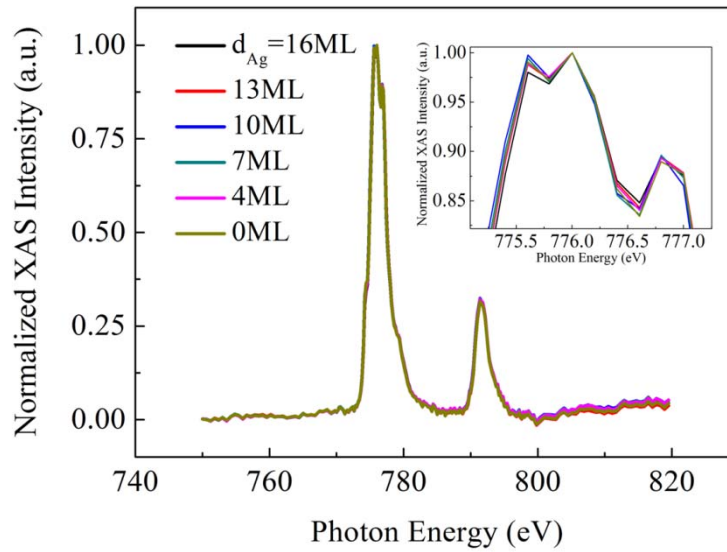


Fig. 4: (color online) X-ray Absorption Spectrum (XAS) from Co 2p level in sample 1. No obvious change in the CoO chemical composition is observed with increasing Ag thickness.

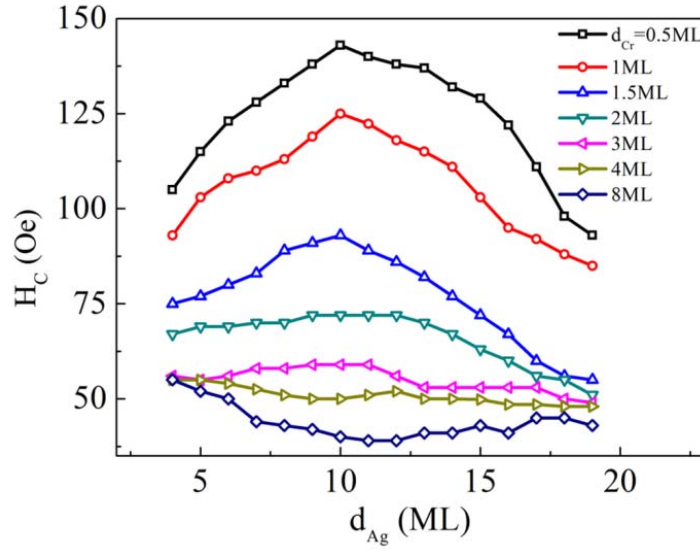


Fig. 5: (color online) Coercivity versus Ag thickness for sample 5. The non-monotonous behavior disappears or shifts peak position with increasing the Cr thickness.

References:

1. W. H. Meiklejohn and C. P. Bean, Phys. Rev. **102**, 1413 (1956).
2. J Nogués and Ivan K. Schuller, J. Magn. Magn. Mater. **192**, 203 (1999).
3. N.C. Koon, Phys. Rev. Lett. **78**, 4865 (1997).
4. D. Mauri, H. C. Siegmann, P. S. Bagus, and E. Kay, J. Appl. Phys. **62**, 3047 (1987).
5. A. P. Malozemoff, Phys. Rev. B **35**, 3679 (1987).
6. T. C. Schulthess and W. H. Butler, Phys. Rev. Lett. **81**, 4516 (1998).
7. M. D. Stiles and R. D. McMichael, Phys. Rev. B **59**, 3722 (1999).
8. P. Miltényi, M. Gierlings, J. Keller, B. Beschoten, and G. Güntherodt, U. Nowak, and K. D. Usadel, Phys. Rev. Lett. **84**, 4224 (2000).
9. Miguel Kiwi, J. Magn. Magn. Mater. **234**, 584 (2001).
10. M. G. Blamire, M. Ali, C.-W. Leung, C. H. Marrows, and B. J. Hickey, Phys. Rev. Lett. **98**, 217202 (2007).
11. S. Maat, K. Takano, S. S. Parkin, and Eric E. Fullerton, Phys. Rev. Lett. **87**, 087202 (2001).
12. H. Ouyang, K.-W. Lin, C.-C. Liu, Shen-Chuan Lo, Y.-M. Tzeng, Z.-Y. Guo, and J. van Lierop, Phys. Rev. Lett. **98**, 097204 (2007).
13. X. P. Qiu, D. Z. Yang, S. M. Zhou, R. Chantrell, K. O'Grady, U. Nowak, J. Du, X. J. Bai, and L. Sun, Phys. Rev. Lett. **101**, 147207 (2008).
14. T. Hauet, J. A. Borchers, Ph. Mangin, Y. Henry, and S. Mangin, Phys. Rev. Lett. **96**, 067207 (2006).
15. Steven Brems, Kristiaan Temst, and Chris Van Haesendonck, Phys. Rev. Lett. **99**, 067201 (2007).
16. S. K. Mishra, F. Radu, H. A. Dürr, and W. Eberhardt, Phys. Rev. Lett. **102**, 177208 (2009).
17. J. Sort, A. Hoffmann, S.-H. Chung, K. S. Buchanan, M. Grimsditch, M. D. Baró, B. Dieny, and J. Nogués, Phys. Rev. Lett. **95**, 067201 (2005).
18. Jung-Il Hong, Titus Leo, David J. Smith, and Ami E. Berkowitz, Phys. Rev. Lett. **96**, 117204 (2006).
19. Marian Fecioru-Morariu, Syed Rizwan Ali, Cristian Papusoi, Martin Sperlich, and Gernot Güntherodt, Phys. Rev. Lett. **99**, 097206 (2007).
20. R. Morales, Zhi-Pan Li, J. Olamit, Kai Liu, J. M. Alameda, and Ivan K. Schuller, Phys. Rev. Lett. **102**, 097201 (2009).
21. Luc Thomas, Andrew J. Kellock, and Stuart S. P. Parkin, J. of Appl. Phys. **87**, 5061

-
- (2000).
22. T. Mewes, B. F. P. Roos, S. O. Demokritov, and B. Hillebrands, *J. of Appl. Phys.* **87**, 5064 (2000).
 23. Z. Q. Qiu and N. V. Smith, *J. of Physics: Condensed Matter* **14**, R169, (2002).
 24. N. J. Gökemeijer, T. Ambrose, and C. L. Chien, *Phys. Rev. Lett.* **79**, 4270 (1997).
 25. M. Gruyters, M. Gierlings, and D. Riegel, *Phys. Rev. B* **64**, 132401 (2001).
 26. V. K. Valev, M. Gruyters, A. Kirilyuk, and Th. Rasing, *Phys. Rev. Lett.* **96**, 067206 (2006).
 27. Zhu-Pei Shi, P. M. Levy and J. L. Fry, *Europhys. Lett.* **26**, 473 (1994).
 28. M. Gierlings, M.J. Prandolini, M. Gruyters, T. Funk, D. Riegel, and W.d. Brewer, *Eur. Phys. J. B* **45**, 137–146 (2005).
 29. P. S. Normile, J. A. De Toro, T. Muñoz, J. A. González, J. P. Andrés, P. Muñoz, R. E. Galindo, and J. M. Riveiro, *Phys. Rev. B* **76**, 104430 (2007).
 30. Young-Yeal Song, Dong-Hyun Kim, Seong-Cho Yu, Petr. D. Kim, Igor Alexandrovic Turpanov, Liudmila Alexeevna Lee, Afanasy Egorovic Buzmakov, and Kyu Won Lee, *J. Appl. Phys.* **103**, 07C112 (2008).
 31. Nghi Q. Lam, Steven J. Rothman, and L. J. Nowicki, *J. Electro-Chem. Soc.* **119**, 715 (1972).
 32. J. Wu, J. S. Park, W. Kim, E. Arenholz, M. Liberati, A. Scholl, Y. Z. Wu, Chanyong Hwang, and Z. Q. Qiu, *Phys. Rev. Lett.* **104**, 217204 (2010).
 33. C. Tusche, H. L. Meyerheim, N. Jedrecy, G. Renaud, A. Ernst, J. Henk, P. Bruno, and J. Kirschner, *Phys. Rev. Lett.* **95**, 176101 (2005).
 34. R. Abrudan, J. Miguel, M. Bernien, C. Tieg, M. Piantek, J. Kirschner, and W. Kuch, *Phys. Rev. B* **77**, 014411 (2008).
 35. F. M. F. de Groot, J. C. Fuggle, B. T. Thole, and G. A. Sawatzky, *Phys. Rev. B* **42**, 5459 (1990).
 36. Hong Li and B.P. Tonner, *Phys. Rev. B* **40**, 10241 (1989).
 37. P. Steadman, C. Norris, C. L. Nicklin, N. Jones, and J. S. G. Taylor, S. A. de Vries, S. L. Bennett, *Phys. Rev. B* **64**, 245412 (2001).
 38. M. D. Stiles, *J. of Mag. Magn. Mat.* **200**, 322 (1999).
 39. Z. Q. Qiu and N. V. Smith, *J. of Physics: Condensed Matter* **14**, R169 (2002).
 40. J. J. Paggel, T. Miller, and T.-C. Chiang, *Science* **283**, 1709 (1999).
 41. Dongqi Li, J. Pearson, S. D. Bader, E. Vescovo, D.-J. Huang, and P. D. Johnson, and B. Heinrich, *Phys. Rev. Lett.* **78**, 1154 (1997).

-
- 42. D. E. Büurgler, F. Meisinger, C. M. Schmidt, D. M. Schaller, H.-J. Güntherodt, and P. Grünberg, *Phys. Rev. B* **60**, R3732 (1999).
 - 43. Z. D. Zhang, Hyuk. J. Choi, R. K. Kawakami, Enresto Escorcia-Apericio, Martin Bowen, Jason Wolfe, E. Rotenberg, N.V. Smith, and Z. Q. Qiu, *Phys. Rev. B* **61**, 76 (2000).